ISBN: 978-3-95450-247-9 ISSN: 2673-5490 doi: 10.18429/JACoW-IPAC2024-MOPR53

INSTABILITY OF ASYMMETRIC ELECTRON DRIVE BEAMS IN HOLLOW PLASMA CHANNELS

R. Y. U. Legaspi*, J. L. F. Gabayno, Department of Physics, Mapúa University, Manila, Philippines

Abstract

Using hollow plasma channels is one approach to compact positron acceleration, potentially reducing the cost and footprint of future linear colliders. However, it is prone to transverse instabilities since beams misaligned from the channel axis tend to get deflected into the channel boundary. In contrast, asymmetric electron drive beams can tolerate misalignment and propagate stably after the initial evolution, but this has only been reported for short distances. In this work, we use quasi-static particle-in-cell simulations to demonstrate the instability of asymmetric drivers even after splitting into two beamlets and reaching equilibrium. As the driver decelerates, its particles gradually return into the channel, making the driver susceptible to deflection by the transverse dipole mode. To understand this behavior, the transverse motion of an individual beam particle is modeled. Strategies to mitigate this instability are also proposed.

INTRODUCTION

The construction of a plasma-based electron-positron collider could pave the way for precision studies of the Higgs boson and other indirect searches beyond the Standard Model at a relatively reasonable price and compact footprint. Although plasma wakefield acceleration (PWFA) has seen significant progress when it comes to electrons [1–7], positron acceleration remains a challenge due to plasma's asymmetric response to charge [8].

Positron acceleration in hollow plasma channels has been proposed [9, 10] and demonstrated [11], but it is prone to transverse instabilities since beams misaligned from the channel axis tend to get deflected into the boundary by the dipole wakefield mode [12]. The dipole wakefield mode excited by a longitudinal charge slice is given as [12, 13]

$$\vec{W}_{\perp 1} = \lambda(\xi)\hat{W}_{\perp 1}(\xi)[(\langle x\rangle\hat{x} + \langle y\rangle\hat{y})],$$

where $\xi = ct - z$, λ is the linear charge density of the beam, $\hat{W}_{\perp m}$ is a coefficient dependent on the parameters of the channel, and $\langle . \rangle$ is a quantity averaged over all the "selected" particles, typically at a given ξ slice. To mitigate this, the use of asymmetric ($\sigma_x \neq \sigma_y$) electron drive beams in the nonlinear regime was proposed. The transverse asymmetry excites the quadrupole wakefield mode, given as [12, 13]

$$\vec{W}_{\perp 2} = \lambda(\xi)\hat{W}_{\perp 2}(\xi)\left[\langle x^2 - y^2\rangle(\hat{x}x - \hat{y}y) + \langle 2xy\rangle(\hat{x}y + \hat{y}x)\right],$$

which defocuses the beam along its wider axis and focuses it along its other transverse axis. This eventually splits the beam into two beamlets at opposite sides of the channel, minimizing the influence of the dipole mode and allowing stable propagation without further deflection. Additionally, the electron filament in its wake is suitable for accelerating and focusing a trailing positron beam.

Although the stable propagation of an initially misaligned asymmetric electron beam has been reported [13], this was only numerically demonstrated for distances (40 cm) less than the beam's depletion length (distance until most of the drive beam's energy has been depleted, which is around 120 cm for this case). In this work, we use quasi-static particle-in-cell simulations to demonstrate the instability of asymmetric beams even after splitting into two beamlets and reaching equilibrium. To better understand this behavior, the transverse motion of a single beam particle is modeled. Strategies to mitigate this instability are also proposed.

SIMULATION SETTINGS AND PARAMETERS

Simulations are done with HiPACE++, a quasi-static particle-in-cell code [14]. The plasma has a density of $n_0 \approx 3.11\times10^{16}\,\mathrm{cm}^{-3}$, corresponding to a plasma frequency of $\omega_p = \sqrt{n_0 e^2/\epsilon_0 m_e} \approx 9.949\,\mathrm{THz}$ ($\omega_p^{-1} = 100\,\mathrm{fs}$) and a skin depth of $k_p^{-1} = c/\omega_p = 30\,\mu\mathrm{m}$. The time step size is $\mathrm{d}t = 5\ \omega_p^{-1}$. The inner ($r_0$) and outer ($R_0$) radii of the channel are 50 µm and 150 µm respectively. The simulation domain is $(-6, 6)\times(-6, 6)\times(-12, 0)\,k_p^{-3}$ in $x\times y\times\zeta$, where x and y are the transverse coordinates and $\zeta = z - ct$ is the co-moving longitudinal coordinate. This domain is divided into $1024\times1024\times1024$ cells, corresponding to a resolution of $0.011\times0.011\times0.011\,k_p^{-3}$. The plasma electrons are represented by 16 macroparticles per cell. The simulations are run for 6000 steps, corresponding to the beam propagating for $s = ct = 90\,\mathrm{cm}$ along the channel.

Unless otherwise stated, the electron beam has a mean energy of 5.11 GeV ($\gamma = 10000$), a peak electron density of $n_b = 4.2475\ n_0$ (total charge of 2 nC or 1.248×10^{10} electrons), a tri-Gaussian profile with $\sigma_x = 20\,\mu\mathrm{m}$, $\sigma_y = 10\,\mu\mathrm{m}$, and $\sigma_z = 30\,\mu\mathrm{m}$, and transverse normalized emittances of $\epsilon_{nx} = 20\,\mu\mathrm{m\,rad}$ and $\epsilon_{ny} = 10\,\mu\mathrm{m\,rad}$; this is similar to the drive beam used in Ref. [13]. It is represented by $2^{27} \approx 1.342\times10^8$fixed-weight macroparticles.

NUMERICAL DEMONSTRATION OF INSTABILITY

To demonstrate the instability, we initially misalign the beam centroid from the channel axis by 0.1 µm along the x ($\langle x\rangle_0 = 0.1\,\mu\mathrm{m}$). The propagation of the misaligned beam in the hollow plasma channel is visualized in Fig. 1, and the deflection of the beam centroid is shown in Fig. 2. The deflection along x agrees with Ref. [13]: the centroid off-

* ryulegaspi@mymail.mapua.edu.ph

ISBN: 978-3-95450-247-9 ISSN: 2673-5490 doi: 10.18429/JACoW-IPAC2024-MOPR53

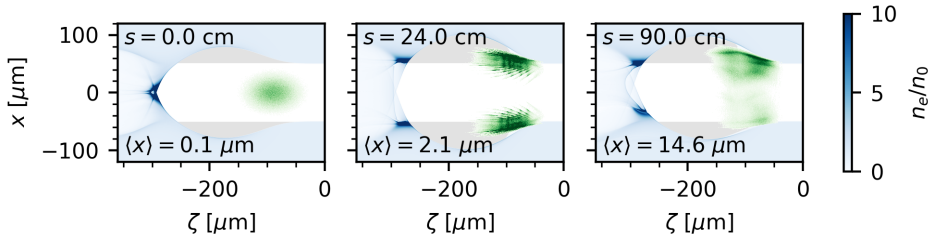

Figure 1: The propagation of a misaligned asymmetric electron beam in a hollow plasma channel. Exposed plasma ions are shown in grey, plasma electrons are shown in blue, and beam electrons are shown in green. These show the x-ζ slices at $y = 0$.

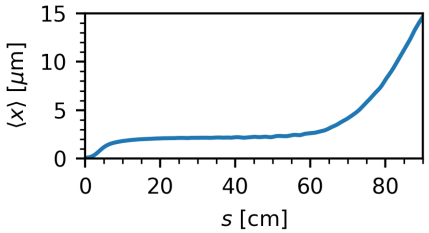

Figure 2: The centroid offset of the beam along x as it propagates for s. The exact final centroid offset may not necessarily converge at higher resolutions, but this sudden deflection at $s \approx 60\,\text{cm}$ is consistent across all simulations so far.

set exponentially increases until the beam splits into two beamlets and reaches equilibrium, saturating at around 2 µm. However, at $s \approx 60\,\text{cm}$, it starts rapidly deflecting again.

To better understand the behavior of the misaligned beam, consider the aligned case ($\langle x \rangle = 0$). The propagation of the aligned beam is visualized in Fig. 3. As the beam propagates through the channel, the quadrupole mode splits the beam along its wider axis into two beamlets. At first, the separation of the two beamlets is distinct. However, as the beam propagates further, the beamlets begin to "smear" and the beam particles gradually get spread throughout the channel. This is quantified in Fig. 4.

This explains the misaligned beam's behavior: as the beam particles return toward the center of the channel, where the dipole mode is dominant, they experience a kick in the direction of the initial offset and get transferred to the beamlet at the opposite side. This starts a feedback loop: the transfer of particles to the other beamlet shifts the beam centroid, which amplifies the dipole mode and promotes the transfer of more particles.

TRANSVERSE MOTION OF A BEAM PARTICLE

But why do the beam particles spread throughout the channel? Consider the relativistic form of Newton's second law:

$$\vec{F} = \frac{\mathrm{d}\vec{p}}{\mathrm{d}t} = \frac{\mathrm{d}}{\mathrm{d}t}\left(\gamma m_0 \vec{v}\right) = m_0 \frac{\mathrm{d}}{\mathrm{d}t}\left(\gamma \vec{v}\right) \tag{1}$$

where γ is the Lorentz factor, m_0 is the particle's rest mass, $\vec{v}$ is its velocity, and $\vec{a}$ is its acceleration. When in a wakefield $\vec{W}$, it experiences a force.

$$\vec{F} = q\vec{W} = m_0 \frac{\mathrm{d}}{\mathrm{d}t}\left(\gamma \vec{v}\right) \tag{2}$$

Here, q is the particle's charge. If we assume the particle to be ultrarelativistic ($v_z \approx c$), then:

$$qW_z = m_0 \frac{\mathrm{d}}{\mathrm{d}t}\left(\gamma v_z\right) = m_0 c \frac{\mathrm{d}\gamma}{\mathrm{d}t} \implies \frac{\mathrm{d}\gamma}{\mathrm{d}t} = \frac{qW_z}{m_0 c} \tag{3}$$

Therefore, a beam particle's equation of motion along x is:

$$qW_x = m_0 \frac{\mathrm{d}}{\mathrm{d}t}\left(\gamma v_x\right) = m_0 \left(\gamma a_x + v_x \frac{\mathrm{d}\gamma}{\mathrm{d}t}\right) \tag{4}$$

$$= m_0 \left(\gamma a_x + v_x \frac{qW_z}{m_0 c}\right) \tag{5}$$

$$a_x = \frac{1}{\gamma m_0}\left(qW_x - qW_z \frac{v_x}{c}\right) \tag{6}$$

The same derivation applies for motion along y.

What does Eq. (6) imply? Suppose a beam particle is experiencing a decelerating wakefield ($qW_z < 0$). If v_x (v_y) and a_x (a_y) have the same sign, then the second term augments the transverse acceleration of the particle. If they have the opposite signs, the second term instead hinders the transverse deceleration of the particle. This means that if an ultrarelativistic particle is decelerating and is subject to (not necessarily linear) focusing forces, then its transverse oscillations tend to increase in amplitude.

Table 1: The parameters and initial conditions (IC) used to solve Eq. (6)

Parameter	Value	IC	Value
W_z	$4.25\,\text{GV m}^{-1}$	γ_0	10000
q	$-e$	x_0	15 µm
m_0	m_e	$v_{x,0}$	0

To validate Eq. (6), we tracked the motion of an individual beam particle in the particle-in-cell simulation and compared it with the equation's prediction given the parameters and initial conditions in Table 1. For this model, we defined the transverse wakefield W_x to be:

$$W_x = \begin{cases} -\alpha x, & \text{if } |x| \le r_0 \\ \frac{en_0}{2\epsilon_0}\left(x - \frac{r_0^2}{x}\right) - \alpha r_0, & \text{if } |x| > r_0 \end{cases} \tag{7}$$

ISBN: 978-3-95450-247-9 ISSN: 2673-5490 doi: 10.18429/JACoW-IPAC2024-MOPR53

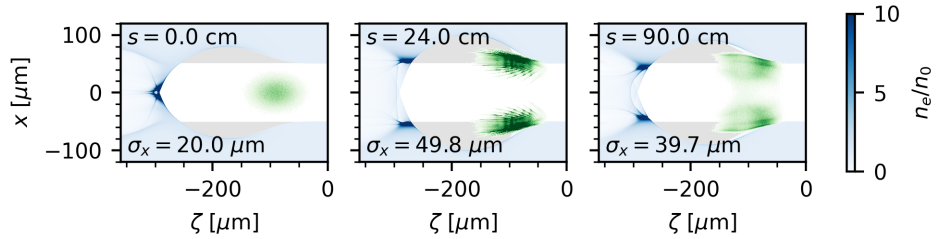

Figure 3: The propagation of an aligned asymmetric electron beam in a hollow plasma channel.

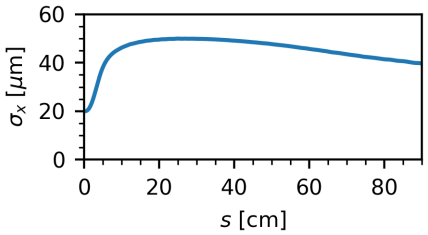

Figure 4: The σ_x of the whole beam as it propagates through the channel. Since σ_x is used to quantify how spread out the beam particles are along x, its decrease corresponds to the return of the beam particles toward the center.

The first condition models the quadrupole mode in the channel, while the second condition models the restoring force exerted by the exposed ions at the channel boundary. α is a coefficient determining the strength of the modeled quadrupole mode. We used $\alpha = 3060\,\mathrm{GV/m^2}$ for $s \leq 9\,\mathrm{cm}$ and $\alpha = 30\,600\,\mathrm{GV/m^2}$ for $s > 9\,\mathrm{cm}$, but this may be determined from the simulation itself for a better prediction.

Figure 5 shows that although the simulation and the prediction do not exactly match, Eq. (6) still captures the most essential behavior: the gradual drift toward the center of the channel ($x = 0$). Ths discrepancy can be attributed to the inaccurate model of the quadrupole mode, especially since it changes with the transverse asymmetry of the beam.

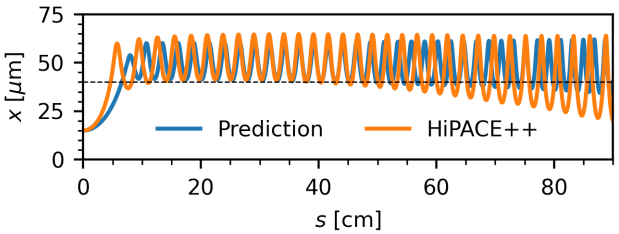

Figure 5: Comparing the particle motion predicted by Eq. (6) and the motion of a particle in the beam's center slice ($\zeta = -90\,\mu\mathrm{m}$) in Fig. 3. The dashed line at $x = 40\,\mu\mathrm{m}$ is for assisting in discerning the amplitude increase of the oscillations.

POTENTIAL MITIGATION STRATEGIES

The second term $(-qW_z\frac{v_x}{c})$ in Eq. (6) implies that for as long as a decelerating wakefield exists at the beam, the instability is unavoidable. However, one potential mitigation strategy is making this term less significant compared to W_x. The quadrupole mode can be enhanced by using flatter, more asymmetric beam profiles. However, increasing the rms momentum spread along the beam's wider axis may be more effective, as shown in Fig. 6. This is because the beam head diverges faster on its own, becoming asymmetric faster and creating a more intense quadrupole mode in its wake.

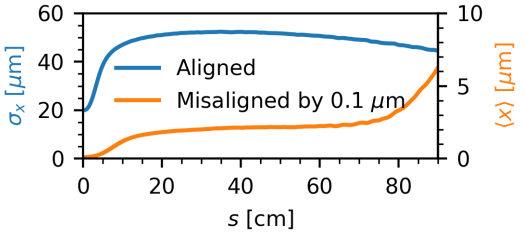

Figure 6: The behavior of an asymmetric beam with varied rms momentum spread. This beam is similar to the previous ones, but it has $\epsilon_{nx} = 25\,\mu\mathrm{m\,rad}$ ($\sigma_{p_x} = 1.25 m_e c$). Notice that the sudden deflection is delayed to $s \approx 75\,\mathrm{cm}$ and is smaller than before. A sufficiently high σ_{p_x} may even eliminate deflection completely within the depletion length.

CONCLUSION

In this work, we have demonstrated the instability of a misaligned asymmetric electron beam at longer propagation distances. We have identified its cause to be beam particles returning to the center of the channel, making it susceptible to deflection by the dipole mode. To better understand this behavior, the transverse motion of an individual beam particle was modeled and then compared to particle-in-cell simulations, with general agreement. We have also presented a potential mitigation strategy, which is by increasing the rms momentum spread of the beam along its wider axis. This makes the head of the beam diverge faster, creating a more intense quadrupole wakefield mode in its wake. Future works could explore other mitigation strategies, such as decreasing the longitudinal wakefield at the drive beam.

ACKNOWLEDGEMENTS

The authors of this work would like to thank Claire Hansel for her useful discussions. This work also used computational resources of the Photonics Research Group, National Institute of Physics, University of the Philippines - Diliman.

ISBN: 978-3-95450-247-9 ISSN: 2673-5490 doi: 10.18429/JACoW-IPAC2024-MOPR53

REFERENCES

[1] P. Chen, J. M. Dawson, R. W. Huff, and T. Katsouleas, "Acceleration of electrons by the interaction of a bunched electron beam with a plasma," *Phys. Rev. Lett.*, vol. 54, pp. 693–696, Jul. 1985. doi:10.1103/PhysRevLett.54.693

[2] N. Barov, J. B. Rosenzweig, M. E. Conde, W. Gai, and J. G. Power, "Observation of plasma wakefield acceleration in the underdense regime," *Phys. Rev. ST Accel. Beams*, vol. 3, p. 011 301, Jan. 2000. doi:10.1103/PhysRevSTAB.3.011301

[3] P. Muggli *et al.*, "Meter-scale plasma-wakefield accelerator driven by a matched electron beam," *Phys. Rev. Lett.*, vol. 93, p. 014 802, Jan. 2004. doi:10.1103/PhysRevLett.93.014802

[4] M. J. Hogan *et al.*, "Multi-gev energy gain in a plasma-wakefield accelerator," *Phys. Rev. Lett.*, vol. 95, p. 054 802, May 2005. doi:10.1103/PhysRevLett.95.054802

[5] I. Blumenfeld *et al.*, "Energy doubling of 42 gev electrons in a metre-scale plasma wakefield accelerator," *Nature*, vol. 445, no. 7129, pp. 741–744, 2007.

[6] M. Litos *et al.*, "High-efficiency acceleration of an electron beam in a plasma wakefield accelerator," *Nature*, vol. 515, no. 7525, pp. 92–95, 2014.

[7] C. A. Lindstrøm *et al.*, "Energy-spread preservation and high efficiency in a plasma-wakefield accelerator," *Phys. Rev. Lett.*, vol. 126, p. 014 801, Jan. 2021. doi:10.1103/PhysRevLett.126.014801

[8] S. Lee, T. Katsouleas, R. G. Hemker, E. S. Dodd, and W. B. Mori, "Plasma-wakefield acceleration of a positron beam," *Phys. Rev. E*, vol. 64, p. 045 501, Apr. 2001. doi:10.1103/PhysRevE.64.045501

[9] T. C. Chiou and T. Katsouleas, "High beam quality and efficiency in plasma-based accelerators," *Phys. Rev. Lett.*, vol. 81, pp. 3411–3414, Oct. 1998. doi:10.1103/PhysRevLett.81.3411

[10] W. D. Kimura, H. M. Milchberg, P. Muggli, X. Li, and W. B. Mori, "Hollow plasma channel for positron plasma wakefield acceleration," *Phys. Rev. ST Accel. Beams*, vol. 14, p. 041 301, Apr. 2011. doi:10.1103/PhysRevSTAB.14.041301

[11] S. Gessner *et al.*, "Demonstration of a positron beam-driven hollow channel plasma wakefield accelerator," *Nature Commun.*, vol. 7, no. 1, p. 11 785, 2016.

[12] C. B. Schroeder, D. H. Whittum, and J. S. Wurtele, "Multimode analysis of the hollow plasma channel wakefield accelerator," *Phys. Rev. Lett.*, vol. 82, pp. 1177–1180, Jun. 1999. doi:10.1103/PhysRevLett.82.1177

[13] S. Zhou *et al.*, "High efficiency uniform wakefield accelera-tion of a positron beam using stable asymmetric mode in a hollow channel plasma," *Phys. Rev. Lett.*, vol. 127, p. 174 801, Oct. 2021. doi:10.1103/PhysRevLett.127.174801

[14] S. Diederichs *et al.*, "Hipace++: A portable, 3d quasi-static particle-in-cell code," *Computer Physics Communications*, vol. 278, p. 108 421, 2022. doi:https://doi.org/10.1016/j.cpc.2022.108421